

SEASONALITY OF PATHFINDER AVHRR LAND NDVI DATA FOR NORTHEASTERN BRAZIL

HUMBERTO ALVES BARBOSA

ALFREDO RAMON HUETE

SWES - Department of Soil, Water and Environmental Sciences, University of Arizona
P. O. Box 210038 – Tucson, Arizona, USA
{humberto, ahuete}@ag.arizona.edu

Abstract. The Normalized Difference Vegetation Index (NDVI) was used to characterize the seasonal variation of land cover over the Northeastern Brazil (NEB) with the NOAA/NASA Pathfinder AVHRR Land (PAL) data set. Twenty years of monthly spatial-aggregated NDVI climatology was determined by calculating lower, mean, and upper NDVI values using a 0.5° lat by 0.5° long grid cell size. The results indicated that the threshold NDVI values of lower and upper phenological activity are 0.103 and 0.771 over NEB, respectively. In this study it was also found that the distribution of NDVI frequency values ranged from 34% (peak centered at 0.3) to 51% (peak centered at 0.7) in May and from 40% (peak centered at 0.3) to 42% (peak centered at 0.7) in October. The seasonal variation of lower and mean NDVI values reflected a better discriminator of the changes of NDVI related to rainy and dry seasons.

Keywords: NDVI, seasonal, threshold.

1. Introduction

The objective of this study was to use the 20-year monthly composites from NOAA/NASA Pathfinder AVHRR Land (PAL) data set at the regional scale in order to characterize the seasonal cycle of lower, mean, and upper Normalized Difference Vegetation Index (NDVI) values over Northeastern Brazil (NEB).

The NDVI calculated from data acquired by the Advanced Very High Resolution Radiometer (AVHRR) sensor on board National Oceanographic and Atmospheric Administration (NOAA) series of satellite has been used as a proxy measure for precipitation in various studies at the local and regional scale over Northeastern Brazil (Barbosa, 1998; Liu and Négron Juárez, 2001). Since its development by Rouse et al. (1973), and its application to Landsat MSS data by Tucker (1979), the NDVI has been used extensively in a variety of studies (Malo and Nicholson, 1990). The NDVI equation is calculated as the normalized ratio between visible and near-infrared reflectance sensed by NOAA-AVHRR, and when integrated over time is related to green biomass.

In NEB, the classification of land cover ranges from Caatinga Arbustiva Aberta (Open Shrubs Shrubbery) to Floresta Ombrófila Densa (Dense Forest) (IBGE, 1993). The dominant characteristic in this region is its marked seasonality which is represented into two seasons, one extending from February through June, and the other from July through January (Kouski and Chu, 1978). These seasons are referred to rainy and dry seasons. Due to the major fluctuations of the weather regime, the onset of the rainy season in this region rapidly initiates a dense increase in leaf and vegetation cover, while the subsequent severe water deficits cause the leaves to shed and the vegetation to die back. Characterization of the seasonal variation of land cover over NEB can be achieved utilizing a 20-year Normalized Difference Vegetation Index (NDVI) from NOAA/NASA Pathfinder AVHRR Land (PAL) data set.

2. Data and Methodology

The NDVI data set used in this study was acquired from the Goddard Distributed Active Archive Center (DAAC) website (<http://daac.gsfc.nasa.gov>) and was provided by the GAC

Pathfinder AVHRR Land Program (PAL) (James and Kalluri, 1994). The GAC Pathfinder NDVI data set is derived from the NOAA AVHRR sensor, which is composited from daily data. The AVHRR sensor was designed for meteorological purposes at 1 km spatial and daily temporal resolution coverage of the Earth's surface. The PAL data used are averaged into 8 km by 8 km pixels and composited over a 30-day period by selecting each pixel from the day with the highest NDVI value, skipping pixels viewed more than 42° from nadir (Holben 1986; Los et al., 1994). The PAL NDVI data set is first processed for various factors such as pre-launch calibration and intra-sensor degradation. It is then normalized for changes in solar zenith angle and corrected for ozone absorption using data from the Total Ozone Mapping Spectrometer (TOMS) as well as correction for Rayleigh scattering (Gordon et al., 1988). Although the PAL NDVI data has been greatly improved, noticeable errors remain including effects of volcanic aerosols, background soil color, water vapor and occasional missing values due to the satellite drifting.

In this study, the PAL NDVI monthly composite data was utilized over the period from September 1981 to September 2001. The 20-year GAC Pathfinder AVHRR NDVI data set for South America was downloaded from the DAAC website, and the data monthly image files were created in 8-bit format in order to facilitate quick visualization of the NDVI data with Environment for Visualizing Images (ENVI) and further rescaled into geophysical meaningful values. The data was originally in the Goode's Interrupted Homolosine projection, and then was geo-referenced in a geographical coordinate system (latitude and longitude) by the authors before being used in this study.

To create the spatial-aggregated NDVI climatology, the NDVI was converted from a satellite grid to a geographical grid with a 0.5° resolution (537 points) for each month from September 1981 to September 2001. The 20-year spatial-aggregated NDVI time series over NEB was used to compute the lower, mean, and upper NDVI values in order to examine the seasonality for each series. For each data set, 20 years of monthly NDVI were processed to compute the seasonal variations of NDVI from January to December. For example, the lower, mean, and upper NDVI seasonal cycles were calculated by averaging the spatial-aggregated NDVI values in January from 1981-01, then averaging the spatial-aggregated NDVI values in February from 1981-01, etc. In addition, we calculated the lower, mean, and upper NDVI frequency distribution at 0.5° grid resolution using 20 years of average-aggregated monthly NDVI values for May (wettest month) and October (driest month). The grid domain used in NEB is located at approximately 1° to 18° S and 35° to 47° W as shown in Figure 1. The gridded NDVI values over NEB were adopted to enable easy comparisons with GCM (Global Circulation Model) forecasts made for this grid. Climatologically, the rainy season of the northern part of NEB is between February and May. This is associated with the southernmost displacement of the Intertropical Convergence Zone (ITCZ). In the southern part of NEB, the rainy season is between December and January (Kouski and Chu, 1978), which is coupled with the South Atlantic Convergence Zone (SACZ).

3. Results

The seasonal patterns of lower, mean, and upper NDVI values were performed on the 0.5° gridded, with monthly resolution from September 1981 to September 2001 in NEB, in order to obtain the structure of seasonal temporal variations of NDVI. Examining the lower and mean NDVI seasonal patterns over NEB for the entire 20-year analysis period, remarkable unimodal seasonal cycles are observed. On an NDVI time profile, both curves are characterized by a strikingly similar pattern that follows a sinusoidal variation as shown in

Figure 2. However, the upper NDVI time profile is characterized by an evenly low seasonal variation. The difference between lower and upper NDVI curves indicates the maximum level of photosynthetic activity (biomass), which is primarily related to spatial and temporal variance in precipitation. Overall, the lower NDVI seasonal cycle is likely related to precipitation conditions while the upper NDVI seasonal cycle is less related to precipitation conditions (Figure 2). The three NDVI curves displayed in Figure 2 capture essential features of the spatial seasonality of greenness for the entire NEB. The rainy and dry changes of NDVI time profile are also evident for the three curves; the green biomass increases up to its maximum value, and then the green biomass progressively decreases.

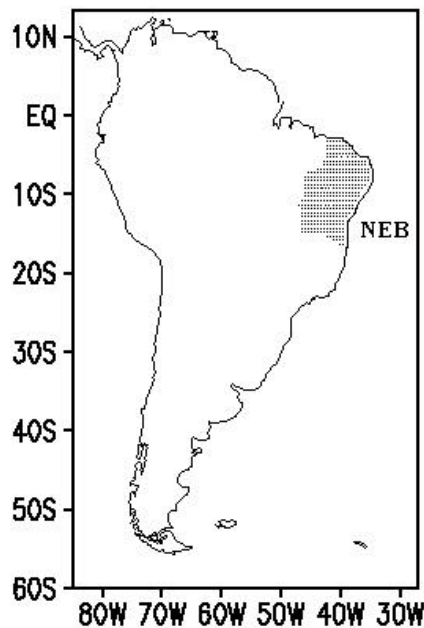


Figure 1. Geographical distribution of the NDVI data points over NEB region.

Among the three curves investigated, the minimum NDVI time profile is highest in March (0.234), April (0.286), May (0.280), June (0.255) and July (0.214), and lowest in October (0.103), November (0.104) and December (0.106). Previous studies have shown that the onset of growing vegetative activity is unlikely to initiate while NDVI value are less than 0.1 (Justice et al., 1986). Mean NDVI time profile is at its highest during the seven-months from January (0.510) through July (0.580) and its lowest from August (0.447) through December (0.459), reaching maximum in May (0.606) and a minimum in October (0.380) corresponding naturally to the rainy and dry seasons. In contrast, the upper NDVI time profile conveys the highest NDVI (0.771) and contributes to sustain its value even during the dry season. A slight decrease of only 11% is observed beginning in September and October to the peak of dry season. The overall picture depicted in Figure 2 suggests that the use of upper NDVI does not provide distinct seasonal variation at the regional scale. The most striking differences among the three curves is the NDVI range values (0.608-0.468) (the difference between the maximum and minimum NDVI values) which remain relatively constant throughout the seasonal cycle, with the upper NDVI limit value (0.771 in May) indicating rainy-season vegetation and the lower NDVI limit value (0.103 in October) defining dry-season vegetation. The spatial variation of NDVI assessed by the coefficient of variation (CV) among the gridded points ranges from 14% to 32%. Not surprisingly, the spatial variation (CV) ranges exhibit the largest values during the dry season.

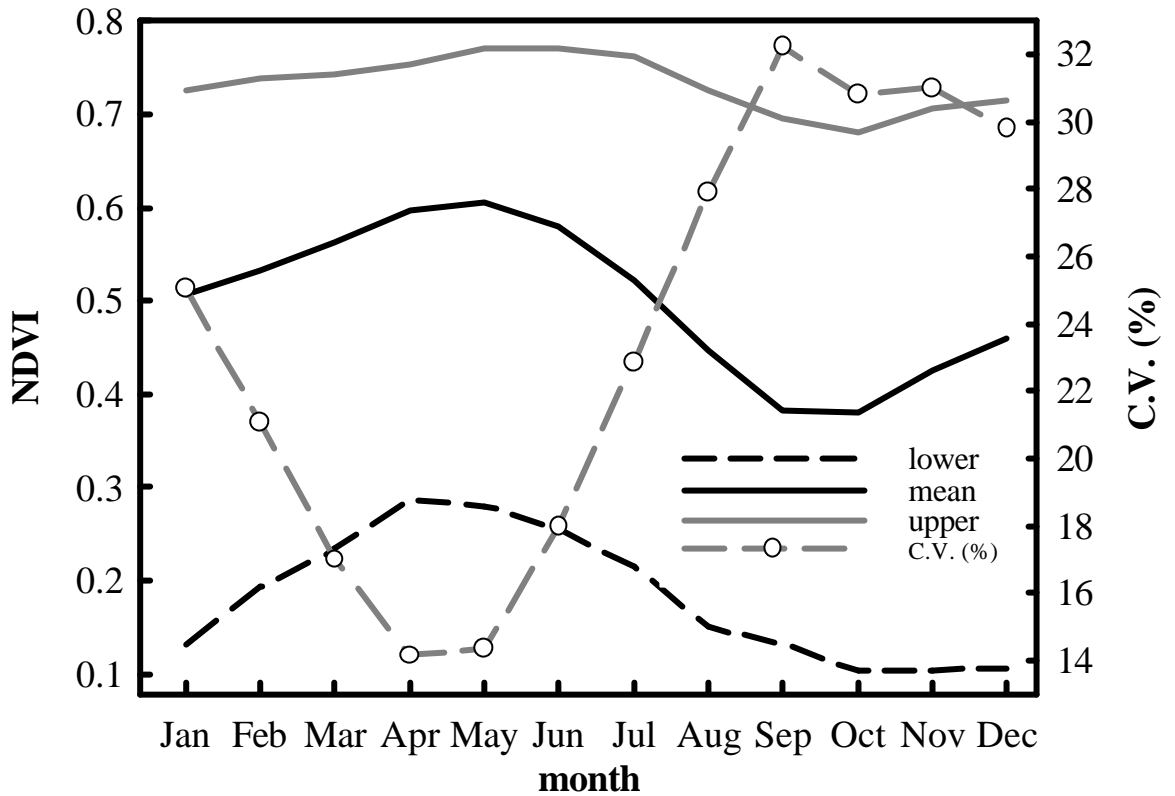


Figure 2. The seasonal variation of monthly spatial-aggregated NDVI climatology (20-yr) for lower limit (dotted line), mean (black solid line), upper limit (gray solid line), and coefficient of variation (CV) over NEB.

To compare months of extreme high and low vegetation over NEB, the lower, mean, and upper frequency distribution of the average-aggregated monthly NDVI at 0.5^0 grid resolution, for May and October were analyzed using 20 years as shown in Figure 3 and Figure 4. The distribution shape for all of the series suggests a normal distribution. In May, the distribution of NDVI frequency patterns exhibit increasing probability trends from lower NDVI frequency curve to upper NDVI frequency curve (Figure 3). On the other hand, the distribution of NDVI frequency patterns in October differ from May; the former displays a relatively similar upper and lower frequency distribution with a sudden downward shift in the mean NDVI frequency curve (Figure 4). The lower and mean NDVI frequency curves for October also have a sharper distribution than the lower and mean NDVI frequency curves for May. In May, the NDVI occurrence frequencies from lower to upper density curves are 34% (peak centered at 0.3), 39% (peak centered at 0.5) and 51% (peak centered at 0.7), respectively. In October, the NDVI occurrence frequencies from lower to upper density curves are 40% (peak centered at 0.3), 37% (peak centered at 0.5) and 42% (peak centered at 0.7), respectively. The mean NDVI frequency curve in May is about 2% less dense than the mean NDVI frequency curve in October.

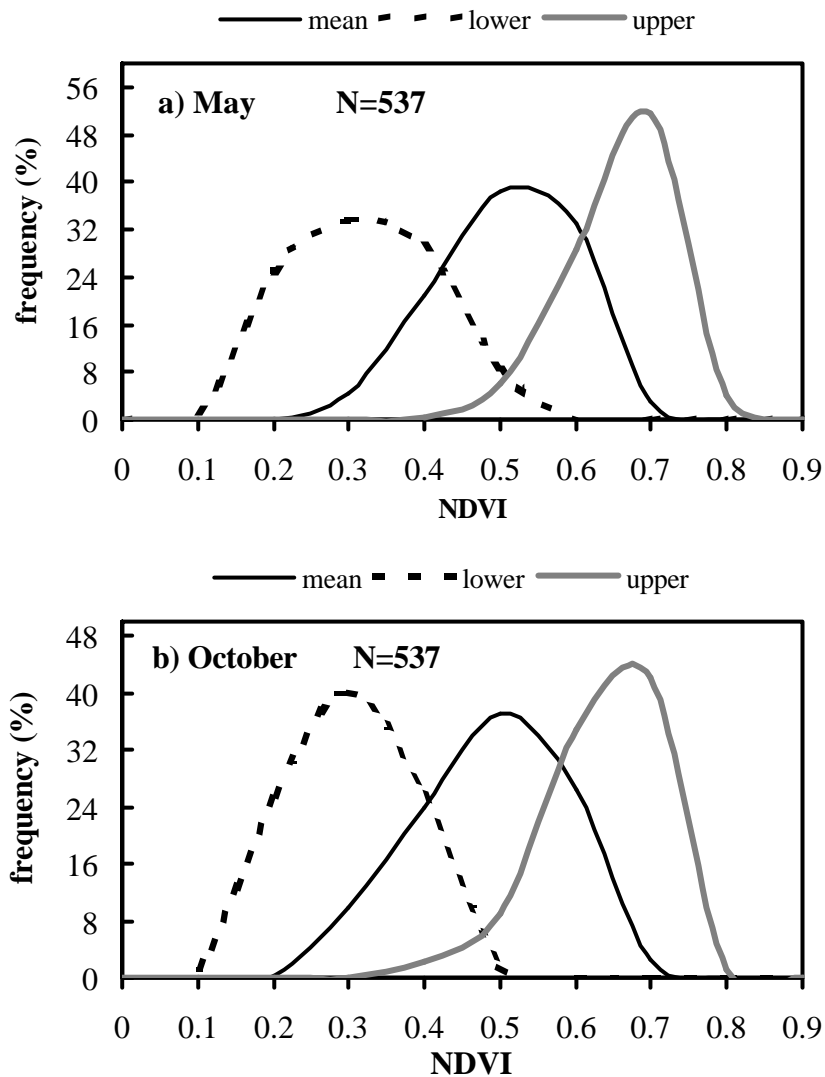


Figure 3. The lower, mean and upper NDVI frequency distribution for (a) May and (b) October.

4. Conclusions

Analysis of twenty years of monthly-gridded NDVI data has resulted in the identification of NDVI thresholds for seasonal variation in the NEB region. In this analysis, the uniformity of spatial and temporal coverage provided by the time scale (monthly) and space scale ($0.5^0 \times 0.5^0$) indicated that there is a large seasonal variation in vegetation cover response due to rainy and dry seasons isolated by the lower, mean, and upper NDVI values at the regional scale. Overall, the results of this study have shown that the NDVI values are scaled between 0.103 and 0.771. The lower threshold NDVI (0.103) represents the dry-vegetated season, and the upper threshold NDVI (0.771) represents the rainy-vegetated season. Thus, NDVI values between the lower threshold (0.103) and upper threshold (0.771) are assigned fractional vegetation values corresponding to the dynamics of vegetation seasonality and different land cover types which are influenced by fluctuations in rainfall over NEB.

In this study, it was also found that the distributions of NDVI frequency values in May for lower NDVI, mean NDVI, and upper NDVI values are 34% (peak centered at 0.3), 39%

(peak centered at 0.5) and 51% (peak centered at 0.7), respectively. In October, the distributions of NDVI frequency values for lower NDVI, mean NDVI, and upper NDVI values are 40% (peak centered at 0.3), 37% (peak centered at 0.5) and 42% (peak centered at 0.7), respectively. The NDVI histograms showed that there are discernible differences for lower and mean NDVI values between May and October, but there are no significant differences for upper NDVI values between May and October. As a result, the lower and mean NDVI values reflect the seasonal climatic fluctuations over NEB.

Acknowledgements

The authors would like to thank the NASA Goddard Space Flight Center for the acquisition of the PAL data.

References

- Barbosa, H. A., 1998. Análises espaço temporal de índice de vegetação AVHRR/NOAA e precipitação na região nordeste do Brasil em 1982-85. São José dos Campos. *Dissertação* (Mestrado em Sensoriamento Remoto) – Instituto Nacional de Pesquisas Espaciais (INPE), pp. 165.
- Gordon, H. R., Brown, J. W., and Evans, R. H., 1988. Exact Rayleigh scattering calculations for use with the Nimbus-7 Coastal Zone Color Scanner, *App. Opt.*, 27, 862-871.
- Holben, B. N., 1986. Characteristics of maximum-value composite images from temporal AVHRR data. *Inter. J. Remote Sensing*, 7, 1417-1434.
- Instituto Brasileiro de Geografia e Estatística (IBGE), 1993. *Recursos Naturais e Meio Ambiente: uma visão do Brasil*. Sueli Sirena Caldeiron – coordenadora. Rio de Janeiro: IBGE, Departamento de Recursos Naturais e Estudos Ambientais, 1993, 154p.
- James, M. E., and Kalluri, S. N. V., 1994. The pathfinder AVHRR land data set: an improved coarse-resolution set for terrestrial monitoring. *Inter. J. Remote Sensing*, 15, 3347-3364.
- Kousky, V. E., and Chu, P. S., 1978. Fluctuations in annual rainfall for northeast Brazil. *J. Meteor. Soc. Japan*, 56, 457-465.
- Liu, W. T., and Negrón Juárez, R. I., 2001. ENSO drought onset prediction in northeast Brazil using NDVI. *Int. J. Remote Sensing*, 22, 17, 3483-3501.
- Justice, C. O., Holben, B. N., and Gwynne, M. D., 1986. Monitoring East African vegetation using AVHRR data. *Int. J. Remote Sensing*, 7, 1453-1474.
- Los, S. O., Justice, C. O., Tucker, C. J., 1994. A global 1°X1° NDVI data set for climate studies derived from the GIMMS continental NDVI data. *Inter. J. Remote Sensing*, 17, 3493-3518.
- Malo, A. R., and Nicholson, S. E., 1990. A study of rainfall and vegetation dynamics in the African Sahel using normalized difference vegetation index. *J. Arid Environ.*, 19, 1-24.
- Prince, J. C., 1991. Timing of NOAA afternoon passes. *Int. J. Remote Sensing*, 12, 193-198.
- Rouse, J. W., Hass, R. H., Schell, J. A., and Deering, D. W., 1973. Monitoring vegetation systems in the great plains with ERTS. *In proceedings*, 3rd ERTS Symposium, 48-62.
- Tucker, C. J., 1979. Red and photographic infrared linear combinations for monitoring vegetation. *Remote Sens. Environ.*, 8, 127-150.